Chemical Science

EDGE ARTICLE

View Article Online
View Journal | View Issue

Cite this: *Chem. Sci.*, 2016, **7**, 4400

A calamitic mesogenic near-infrared absorbing croconaine dye/liquid crystalline elastomer composite†

Ling-Xiang Guo,[a] Mei-Hua Liu,[a] Sayed Mir Sayed,[a] Bao-Ping Lin,[a] Patrick Keller,[bcd] Xue-Qin Zhang,[a] Ying Sun[a] and Hong Yang*[a]

Received 18th February 2016
Accepted 24th March 2016

DOI: 10.1039/c6sc00758a

www.rsc.org/chemicalscience

In this work, we report the first example of a calamitic mesogenic near-infrared (NIR) absorbing organic dye, made by functionalizing a thiophene–croconaine chromophore rigid core with two symmetric long flexible alkyl chains. The liquid crystal (LC) NIR dye **YHD796** exhibits a sharp and intense NIR absorption band with a maximum absorption peak at 796 nm. Taking advantage of the improved solubility of **YHD796** dispersed in mesogenic molecules, a homogeneously-aligned mono-domain liquid crystalline elastomer (LCE)/**YHD796** composite film is successfully prepared by applying the classical LC-cell-alignment method and *in situ* photo-polymerization of photocurable LC monomer mixtures. This LCE/**YHD796** composite film performs a fully reversible contraction/expansion response towards NIR light stimulus due to the photo-thermal heating effect induced by the **YHD796** dye well-dispersed in the LCE matrix.

Introduction

Photoresponsive polymeric materials have garnered significant interest within the last few decades due to their ability to undergo rapid changes in response to light, which compared with other stimuli (*i.e.* pH, heat, electric, magnetic, chemicals, *etc.*), is advantageous to maximize resolution in time and space. This unique physical characteristic endows photoresponsive polymeric materials with prospective applications ranging from medical technology to robotic devices.[1–5] Among them, photo-actuated liquid crystalline elastomers (LCEs) can vary their microscopic mesogenic order by absorbing photon energy to further change the macroscopic material shapes, and thus have received increasingly scientific attention.[6–19]

Traditional photoresponsive LCE materials relying on the *trans–cis* isomerization effect of incorporated azobenzene chromophores are generally light-stimulated by UV sources (λ < 400 nm). Recently, near-infrared (NIR) light sources (λ > 760 nm) have become more and more popular in photo-responsive systems because of their high biological tissue penetration ability, excellent biocompatibility and broad utility in biomedical applications.[20–24] Up to now, the preparation strategies for NIR-stimulus-responsive LCEs can be divided into two categories: (1) through doping inorganic or organic up-conversion materials into azobenzene-containing LCE materials, IR irradiation can be converted into low-wavelength lights to realize azobenzene *trans–cis* isomerization.[25,26] (2) Taking advantage of the photo-thermal effect of thermally conductive fillers (carbon nanotubes,[27–34] gold nanoparticles,[35–37] *etc.*), photons can be transformed into heat energy, which induces the LC-to-isotropic phase transition and further force the whole sample to actuate macroscopically.

Nowadays, the latter strategy dominates the field of NIR-responsive LCEs due to the benefit of versatile mesogenic structure designs unbound to azobenzene. However the most serious drawback is that most of the dopants are inorganic nanoparticles, which are usually difficult to disperse in organic LCE matrixes,[33] naturally weaken the matrix mechanical properties and slow down the photo-actuation response of the prepared LCE composites.[34] An ideal solution could be to use organic IR absorbing dyes, which follow non-radiative relaxation pathways to realize the photo-thermal heating.

However, IR dyes are relatively rare species and most of the previously reported organic dye/LCE composites were sensitive to UV-vis light with wavelengths ranging from 300 to 650 nm.[38–40] Up to now, the only two NIR absorbing dyes used in LCEs have been BASF Lumogen IR788 (ref. 41 and 42) (CAS no. 333304-54-4 (ref. 43 and 44)) and Dye 1002.[32] As shown in Fig. 1, Lumogen IR788 is a quaterrylenetetracarboxylic diimide IR absorbent with a complicated polyaromatic structure, which unfortunately has a poor solubility in certain photocurable

[a]*School of Chemistry and Chemical Engineering, Jiangsu Province Hi-Tech Key Laboratory for Bio-medical Research, Jiangsu Optoelectronic Functional Materials and Engineering Laboratory, Southeast University, Nanjing, 211189, China. E-mail: yangh@seu.edu.cn; Tel: +86-25-52090620*

[b]*Institut Curie, PSL Research University, CNRS, UMR 168, F-75005 Paris, France*

[c]*Sorbonne Universités, UPMC Univ Paris 06, CNRS, UMR 168, F-75005 Paris, France*

[d]*Soft Materials Research Center and Department of Chemistry and Biochemistry, University of Colorado, Boulder, CO 80309, USA*

† Electronic supplementary information (ESI) available: Instrumentation descriptions, synthetic protocols, NMR spectra and a NIR-responsive video (S1.avi). See DOI: 10.1039/c6sc00758a

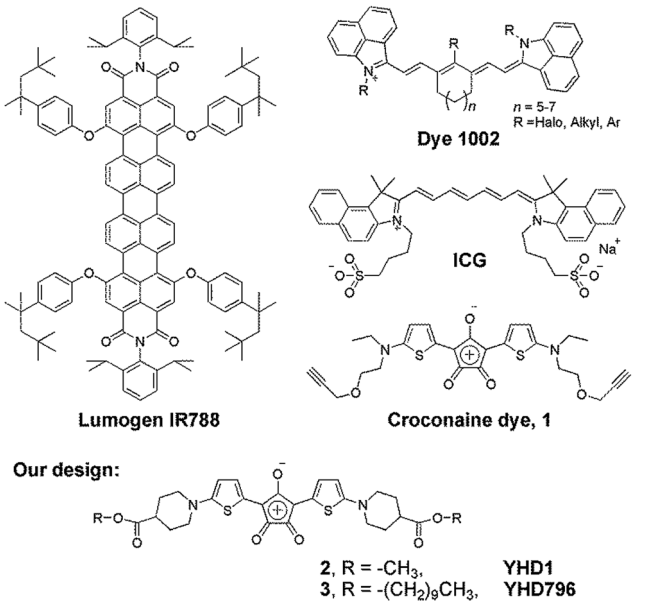

Fig. 1 The molecular structures of Lumogen IR788, Dye 1002, ICG, Smith's croconaine dye and the LC-like NIR absorbing dyes (**YHD1** and **YHD796**) reported in this manuscript.

liquid crystal (LC) monomers based on our initial trials, while the maximum filling content of Dye 1002 was 0.2 wt% based on literature report.[32] This limitation prompted us to look for an alternative IR-absorbing compound with optimal solubility in LCE matrix. Based on like-dissolve-like theory, a calamitic mesogenic NIR absorbing dye was our objective.

Our design was inspired by Smith's croconaine dye[45] (compound **1**, Fig. 1) which compared with the most-studied indocyanine green (ICG, Fig. 1) dye, had "an intense absorption band, very short singlet excited state lifetime with highly efficient relaxation to the ground state, negligible intersystem crossing to triplet state and very low oxygen photosensitization ability, high chemical and thermal stability".[45] Most importantly, the thiophene–croconaine chromophore was potentially a perfect rigid mesogenic core for building calamitic LC molecular structures. Based on this design logic, we decorated the thiophene–croconaine core with two symmetric isonipecotates bearing different alkyl tails ($-C_nH_{2n+1}$, $n = 1$ or 10) to synthesize two LC-like NIR absorbing dyes (**YHD1**, **YHD796**, Fig. 1).

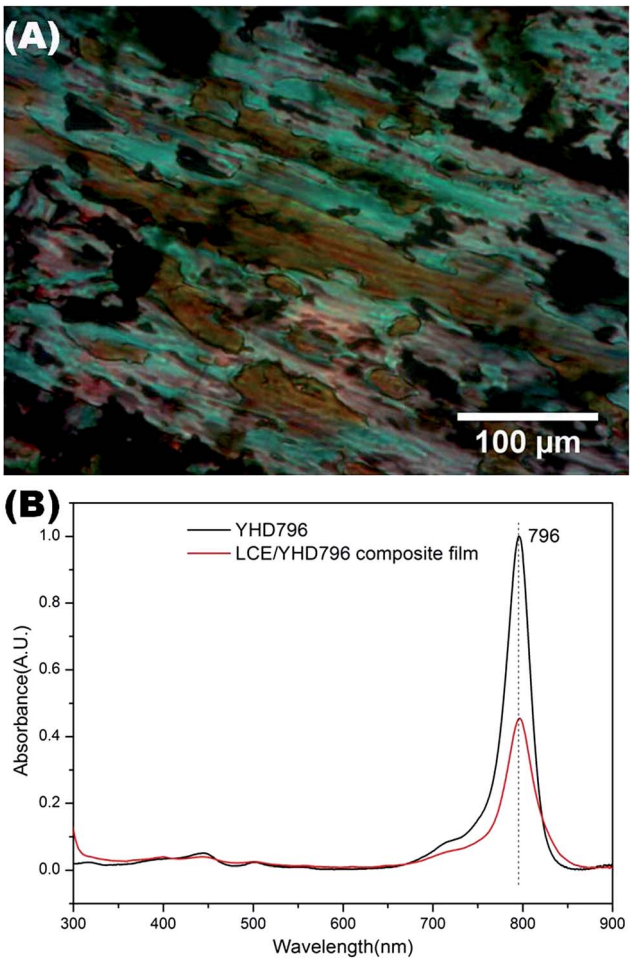

Fig. 2 (A) Polarized optical microscope image of **YHD796** recorded at 110 °C. (B) UV-vis absorption spectra of **YHD796** (conc. = 2.98×10^{-3} mg mL^{-1}, dissolved in CH_2Cl_2) and LCE/**YHD796** composite film (conc. = 0.11 mg mL^{-1}, swelled in CH_2Cl_2) measured at 25 °C.

Experimental section

General considerations

The LC monomer **A444** was synthesized following our previous report.[46–49] All the detailed instrumentation descriptions, synthetic protocols, and NMR spectra are described in the ESI.†

Synthesis of 1-thiophen-2-yl-piperidine-4-carboxylic acid (8)

Compound **6** (1.00 g 4.45 mmol) and 25 mL of 0.5 N sodium hydroxide solution were added into a 100 mL round-bottom flask. The reaction mixture was heated at reflux temperature for 3 h. After cooling to room temperature, the mixture was acidified with 10 mL of aqueous acetic acid (conc. 10%). The precipitate was collected by filtration and dried under vacuum, to give intermediate **8** as a white solid (0.76 g, yield 80.8%). ^{1}H NMR (300 MHz, $CDCl_3$) δ: 6.78 (dd, J = 6.0, 3.0 Hz, 1H), 6.61 (d, J = 6.0 Hz, 1H), 6.14 (d, J = 3.0 Hz, 1H), 3.52 (m, 2H), 2.94–2.76 (m, 2H), 2.48 (m, 1H), 1.96 (m, 4H). ^{13}C NMR (75 MHz, $CDCl_3$) δ: 179.74, 160.59, 126.03, 112.55, 105.93, 51.45, 40.08, 27.36.

Synthesis of 1-thiophen-2-yl-piperidine-4-carboxylic acid decyl ester (9)

Compound **8** (0.76 g, 3.60 mmol), *n*-decyl alcohol (0.68 g, 4.34 mmol), DMAP (0.02 g, 0.18 mmol) and dry CH_2Cl_2 (25 mL) were added into a 50 mL Schlenk-type flask. Under a nitrogen atmosphere, DCC (0.88 g, 4.27 mmol) was added into the above flask in one portion at 0 °C, and the reaction solution was stirred at room temperature for 24 h. After filtering off the precipitate, the solution was concentrated by rotary evaporation and the crude oil was purified by column chromatography (petroleum ether : ethyl acetate = 15/1) to give the product **9**

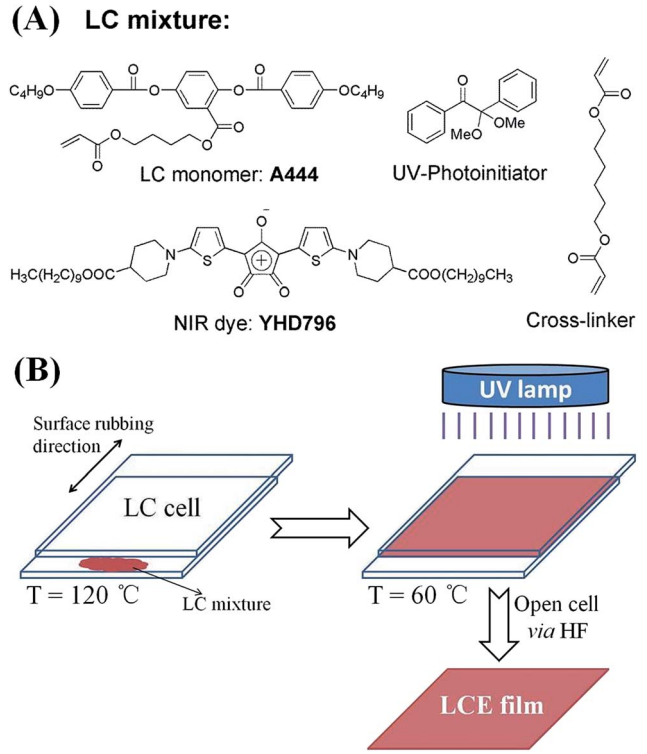

Fig. 3 (A) Molecular structures of photocurable LC mixtures: monomer A444, photoinitiator, crosslinker and NIR dye YHD796. (B) Schematic illustration of homogeneously-aligned LCE/YHD796 composite film preparation protocol.

(0.70 g, yield 55.6%) as a colorless oil. ^{1}H NMR (300 MHz, $CDCl_3$) δ: 6.77 (dd, J = 6.0, 3.0 Hz, 1H), 6.60 (t, J = 6.0 Hz, 1H), 6.13 (m, 1H), 4.16–4.03 (t, J = 8.3 Hz, 2H), 3.51 (m, 2H), 2.84 (m, 2H), 2.42 (m, 1H), 2.07–1.87 (m, 4H), 1.40–1.22 (m, 16H), 0.89 (t, J = 6.6 Hz, 3H). ^{13}C NMR (75 MHz, $CDCl_3$) δ: 174.51, 126.02, 112.31, 105.65, 64.64, 51.55, 40.57, 31.84, 29.60, 28.99, 28.60, 27.66, 25.88, 22.62, 14.04.

Synthesis of 2,5-bis[(decyl-4-carboxylate-piperidylamino) thiophenyl]-croconium (YHD796)

Croconic acid 7 (0.14 g, 0.98 mmol) and compound **9** (0.69 g, 1.96 mmol) were added into a solution of 30 mL toluene/*n*-butanol (v/v, 1/1) under nitrogen atmosphere. The reaction mixture was heated to reflux for 1 h. After cooling to room temperature, the mixture was transferred into a 100 mL round-bottom flask and diluted with 15 mL of dichloromethane. The solution was concentrated by rotary evaporation and the resulting crude black solid was purified by column chromatography (CH_2Cl_2 : methanol = 50/1) to give the desired product **YHD796** (0.64 g, yield 79.9%) as a black solid. ^{1}H NMR (300 MHz, $CDCl_3$) δ: 8.67 (m, 2H), 6.50 (m, 2H), 4.08 (t, J = 8.3 Hz, 4H), 3.89 (m, 4H), 3.41 (m, 4H), 2.63 (m, 2H), 1.95 (m, 8H), 1.65 (m, 4H), 1.26 (m, 28H), 0.85 (t, J = 6.0 Hz, 6H). ^{13}C NMR (75 MHz, $CDCl_3$) δ: 173.21, 141.21, 124.29, 113.00, 65.15, 50.41, 39.71, 31.81, 30.64, 24.09, 22.59, 14.02. ESI-MS m/z: 831.6 $[m + Na]^+$, calculated for **YHD796**: 808.6.

Preparation of LCE/YHD796 composite film

As shown in Fig. 3, LC monomer **A444** (30.11 mg, 4.76×10^{-2} mmol), hexamethylene diacrylate (1.20 mg, 5.29×10^{-3} mmol), 2,2-dimethoxy-2-phenylacetophenone (0.34 mg, 1.33×10^{-3} mmol) and **YHD796** (0.42 mg, 0.53×10^{-3} mmol) were mixed and dissolved in CH_2Cl_2 which was then evaporated to provide the LC mixture. The mixture was filled by capillarity into an antiparallel homogeneous-aligned LC cell with 20 μm gap placed on a hot stage which set the temperature at 120 °C. The LC cell was slowly cooled down to 60 °C at a rate of −1.0 °C per minute and annealed at 60 °C for *ca.* 2 h to achieve a fine planar alignment. A subsequent UV irradiation was carried out under a stream of nitrogen gas (using a zip-lock bag).[50,51] After UV irradiation (365 nm, 20 mW cm^{-2}) for 1.5 h, the LC cell was placed into a 40% hydrofluoric acid solution for 3 days to dissolve the glass cell[52] and give the desired LCE/**YHD796** composite as a free-standing film.

Results and discussion

Syntheses and physical properties of NIR absorbing dyes

The synthetic protocols for the two NIR absorbing dyes (**YHD1** and **YHD796**) are illustrated in Scheme 1. Thiophene-2-thiol (**4**) was first nucleophilically substituted by methyl isonipecotate (**5**) to give intermediate **6**,[53] which was further reacted with croconic acid (7) to provide **YHD1**. To lengthen the alkyl tails of the croconaine dye, intermediate **6** was subjected to a sequential alkaline saponification/acid hydrolysis process and then DCC-coupled with *n*-decyl alcohol to synthesize its long-tail analogue **9**, which was subsequently converted into the corresponding NIR dye **YHD796**.

The mesomorphic properties of **YHD1** and **YHD796** were investigated by polarized optical microscopy (POM). Unsurprisingly, the short-tail dye **YHD1** with a high melting point at 236–237 °C had no LC phase and a poor solubility in mesogenic monomer **A444** (Fig. 3A).[46] Similar to Lumogen IR788, the mixture of **A444** and **YHD1** (1.0 wt%), when filled in LC cells, underwent obvious phase segregation. On the contrary, the long-tail analogue **YHD796** exhibited a monotropic LC mesophase

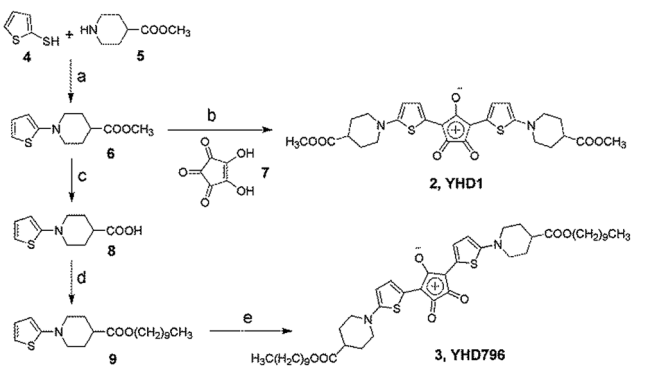

Scheme 1 The synthetic routes of NIR dyes YHD1 and YHD796. Reagents and conditions: (a) toluene, reflux; (b) toluene/*n*-butanol, reflux; (c) NaOH, reflux, then acidified with HOAc; (d) DCC, DMAP, *n*-decyl alcohol; (e) croconic acid 7, toluene/*n*-butanol, reflux.

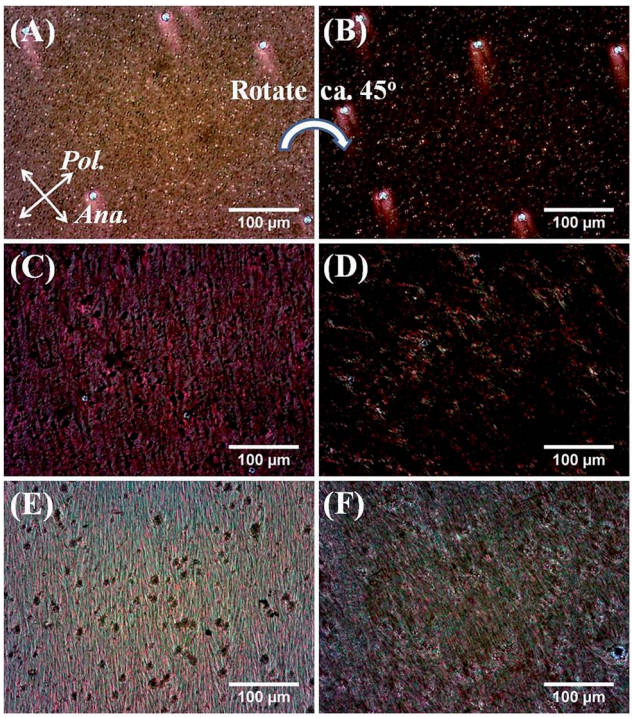

Fig. 4 POM images of **A444**/HMDA/DMPA/**YHD796** mixture filled in a LC cell (A, B) before UV illumination and (C, D) after UV illumination, and (E, F) the corresponding LCE/**YHD796** composite film released from HF-etched LC cell.

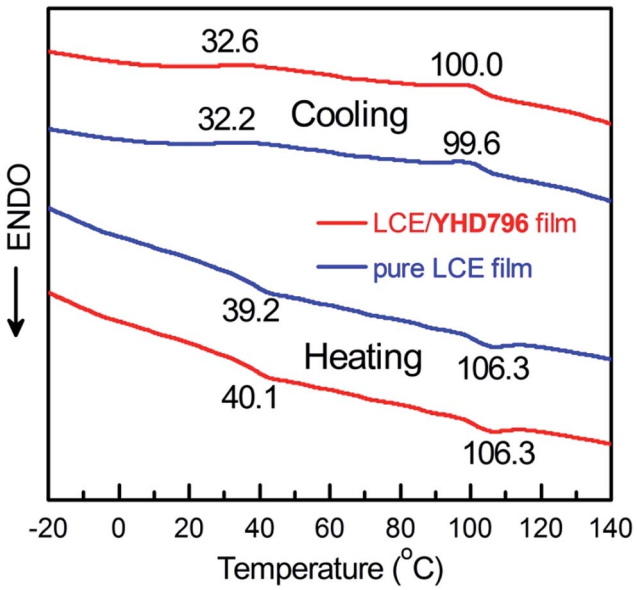

Fig. 5 DSC curves of pure LCE film and LCE/**YHD796** composite film during the first cooling scan and the second heating scan at a rate of 10 °C min^{-1} under nitrogen atmosphere.

(phase sequence and transition temperatures: crystal (K) – 84 °C – nematic (N) – 178 °C – isotropic (I) (on heating); I – 32 °C – K (on cooling)), with a characteristic nematic marble texture as shown in Fig. 2A. The nematic phase was also confirmed by wide-angle X-ray scattering analysis (WAXS, Fig. S16†) which presented no sharp scattering peaks in the low-angle region when **YHD796** sample was heated to a temperature above its melting point (84 °C). Most importantly, due to the two symmetric long flexible alkyl tails, calamitic dye **YHD796** could be well-solubilized in **A444** system (up to *ca.* 10 wt%).

Examined by UV-vis spectroscopy, the mesogenic dye **YHD796** exhibited a very sharp and intense NIR absorption band ($\lambda_{abs,max}$ = 796 nm, conc. = 2.98 × 10^{-3} mg mL^{-1} in CH_2Cl_2), which was consistent with previously reported croconaine dye analogues.[45] Hereinafter, we focused **YHD796** for further investigation and application.

Preparation and photo-responsive behavior of LCE/YHD796 composite film

With this novel mesogenic NIR-absorbing dye in hand, we started to dope **YHD796** into photocurable LC monomer matrix and prepare the corresponding LCE/**YHD796** composite films. In order to achieve a good uniaxial-alignment for synthesizing mono-domain LCE membranes, we chose the widely used LC-cell-alignment method[46,54,55] that relied on the surface anchoring effect of anti-parallel-rubbed polyimide surface layers of LC cells to align the mesogens uniaxially. We further applied *in situ* photo-polymerization reaction to fabricate mono-domain LCE membranes. As shown in Fig. 3A, **YHD796** was mixed with acrylate LC monomer **A444**, the crosslinker hexamethylenediacrylate (HMDA) and the photoinitiator 2,2-dimethoxy-2-phenylacetophenone (DMPA) with a molar ratio of 1.0 : 90 : 10 : 2.5. The LC mixture was then filled into an anti-parallel surface-rubbed LC cell at the temperature above its clearing point. After lowering the temperature to the LC phase, UV-initiated (λ = 365 nm) *in situ* photo-polymerization and photo-crosslinking were executed on the homogeneously-aligned LC mixture. Finally, the LC cell was completely etched in hydrofluoric acid aqueous solution to obtain the free LCE/**YHD796** composite film. The preparation protocol is schematically illustrated in Fig. 3B, and described in details in the Experimental section.

POM technique was applied to investigate the homogeneous-alignment of the LCE/**YHD796** composite film. As indicated in Fig. 4A and B, the photocurable **A444**/HMDA/DMPA/**YHD796** mixture in a LC cell showed the lowest transmittance when the polarizer was parallel or perpendicular to the cell surface rubbing direction. When rotating the cell with an interval of 45°, maximum transmittance was clearly observed. After UV-initiated photo-polymerization, the corresponding LCE/**YHD796** composite film either inside the LC cell (Fig. 4C and D) or released from HF-etched LC cell (Fig. 4E and F) also presented similar light transmittance variation behavior, although the LC birefringences were slightly different from each other in these three stages. Overall, the planar alignment of mesogenic units in mono-domain LCE/**YHD796** composite film was fairly good.

For comparison, we prepared a pure LCE film containing **A444**/HMDA/DMPA with the exact same molar ratio (90/10/2.5) but no **YHD796** dye. As demonstrated in Fig. 5, the DSC curves of the LCE/**YHD796** composite and the pure LCE film both showed an enantiotropic nematic phase in a perfectly matched temperature range of *ca.* 40–106.3 °C, although the N-to-I

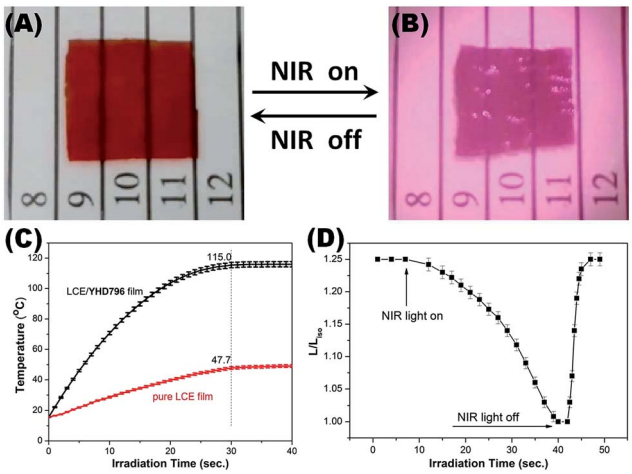

Fig. 6 The images of LCE/**YHD796** composite film under NIR (808 nm) illumination for (A) 0 and (B) 33 seconds. (C) The NIR illumination time *vs.* temperature diagram of LCE/**YHD796** composite film and pure LCE film. (D) The NIR illumination time *vs.* the shape deformation L/L_{iso} of LCE/**YHD796** composite film along the alignment direction.

enthalpy change (1.154 J g^{-1} K^{-1}) of the LCE/**YHD796** composite was slightly higher than the ΔH value (1.081 J g^{-1} K^{-1}) of the pure LCE sample.

The optical absorption of the LCE/**YHD796** composite material was examined by UV-vis spectroscopy. As shown in Fig. 2B, the composite sample had a similar NIR absorption band as the free **YHD796** dye, with a maximum absorption at 796 nm when swelled in CH_2Cl_2 with a concentration of 0.11 mg mL^{-1}. Based on this, the concentration of incorporated **YHD796** dye could be roughly estimated as *ca.* 1.44 × 10^{-3} mg mL^{-1}. However this value might not be accurate since **YHD796** molecule is an ionic salt which might be soluble to some extent in the HF aqueous solution used during the cell-etching process, although the hydrophobic surface properties of LCE films should limit the leaching of NIR dye.

Encouraged by the UV-vis spectrum result, we used a NIR light source (output power: 8 W, center wavelength: 808 ± 3 nm) to investigate the NIR-stimulated photo-actuation characteristics of the LCE/**YHD796** composite film and the pure LCE film. Theoretically, if the embedded NIR dyes could efficiently convert the absorbed photon energy into enough thermal energy to raise the local temperature of mono-domain LCE samples above their T_{ni}, the mesogenic orders would change. Due to the elastic strains and forces provided by the crosslink points in the matrix, a spontaneous and reversible uniaxial shrinkage/expansion of LCE materials along the LC director should be visualized.

As indicated in Fig. 6A and B and Video S1,† the prepared LCE/**YHD796** composite film underwent a rapid shrinking transformation upon NIR illumination and reached maximum contraction in 33 seconds. After NIR source was removed, the LCE composite film fully recovered its original shape. This reversible shrinkage/expansion phenomenon was observed repeatedly during several NIR-light on/off cycles. In contrary, the pure LCE film had no NIR-responsive behavior due to the lack of **YHD796** dye.

In order to further confirm that the shrinking behavior of LCE/**YHD796** composite film under NIR illumination was indeed induced by the photo-thermal heating effect of **YHD796** dye, the surface temperature variations of LCE/**YHD796** composite film and of the pure LCE film as a function of NIR irradiation time were continuously recorded by a thermal imager (FLUKE Ti90). As shown in Fig. 6C, the temperature of the LCE/**YHD796** sample jumped within 30 seconds from 16 °C to 115 °C, higher than its clearing point (T_{ni} = 106.3 °C), while the temperature of the pure LCE film reached a maximum value of *ca.* 47.7 °C in the same period. These data demonstrated that the incorporated **YHD796** dye was the key driving force to achieve the local anisotropic-to-isotropic phase transition in the photo-triggered actuation behavior of the LCE/**YHD796** composite film.

The uniaxial expansion (L/L_{iso}) of the LCE/**YHD796** composite film *versus* NIR illumination time is plotted in Fig. 6D, where L is the length of the LCE composite film along the alignment direction at any specific irradiation time, and L_{iso} is the minimum length of the material in its isotropic state. As indicated in Fig. 6D, the composite film under NIR illumination gradually realized the maximum contraction of *ca.* 25% in 33 seconds, and once the NIR light source was removed, it recovered its original shape in 3–5 seconds. This sharp contrast can be explained by the photo-thermal heating effect, which can only increase the local temperature of the LCE composite sample but not the environmental temperature. Thus as soon as NIR is turned off, the tiny thermal energy generated inside the LCE composite sample is spontaneously and rapidly released into the much colder and larger environment.

Conclusions

In this work, we design and synthesize a calamitic mesogenic NIR absorbing organic dye **YHD796**, by functionalizing a thiophene–croconaine chromophore core with two symmetric long flexible alkyl chains. To the best of our knowledge, this rod-like molecule is the first example of organic dye exhibiting not only a sharp and intense NIR absorption band with a maximum absorption peak at 796 nm but also a LC mesophase. Due to the improved solubility of **YHD796** in mesogenic monomers and the remarkable photo-thermal heating effect, the corresponding LCE/**YHD796** composite film prepared by using the classical LC-cell-alignment method and *in situ* photo-polymerization protocol, performed a fully reversible contraction/expansion response towards NIR light stimulus. Although the mesogenic NIR absorbing organic dye is obviously advantageous to synthesize well dispersed dye/LCE composites, its ionic salt form might bring some challenges when dealing with HF etching or electric field alignment process. Further development of non-ionic mesogenic NIR absorbing organic dyes are under investigation.

Acknowledgements

This research was supported by National Natural Science Foundation of China (Grant No. 21374016) and Priority

Academic Program Development of Jiangsu Higher Education Institutions. P. K. would like to acknowledge the support by the Soft Materials Research Center under NSF MRSEC Grant No. DMR-1420736. We thank Dr Julie Plastino (Curie Institute) for her critical reading of the manuscript.

Notes and references

1 F. D. Jochum and P. Theato, *Chem. Soc. Rev.*, 2013, **42**, 7468–7483.
2 C. Zhu, C. Ninh and C. J. Bettinger, *Biomacromolecules*, 2014, **15**, 3474–3494.
3 Y. Zhao, *Macromolecules*, 2012, **45**, 3647–3657.
4 J. M. Schumers, C. A. Fustin and J. F. Gohy, *Macromol. Rapid Commun.*, 2010, **31**, 1588–1607.
5 P. S. Stayton, T. Shimoboji, C. Long, A. Chilkoti, G. Ghen, J. M. Harris and A. S. Hoffman, *Nature*, 1995, **378**, 472–474.
6 C. Ohm, M. Brehmer and R. Zentel, *Adv. Mater.*, 2010, **22**, 3366–3387.
7 T. Ikeda, J. I. Mamiya and Y. Yu, *Angew. Chem., Int. Ed.*, 2007, **46**, 506–528.
8 H. Yu and T. Ikeda, *Adv. Mater.*, 2011, **23**, 2149–2180.
9 T. J. White and D. J. Broer, *Nat. Mater.*, 2015, **14**, 1087–1098.
10 H. Yang, G. Ye, X. Wang and P. Keller, *Soft Matter*, 2011, **7**, 815–823.
11 M. Warner and E. M. Terentjev, *Prog. Polym. Sci.*, 1996, **21**, 853–891.
12 H. Finkelmann, E. Nishikawa, G. G. Pereira and M. Warner, *Phys. Rev. Lett.*, 2001, **87**, 015501.
13 Y. Yu and T. Ikeda, *Angew. Chem., Int. Ed.*, 2006, **45**, 5416–5418.
14 C. L. van Oosten, C. W. M. Bastiaansen and D. J. Broer, *Nat. Mater.*, 2009, **8**, 677–682.
15 P. M. Hogan, A. R. Tajbakhsh and E. M. Terentjev, *Phys. Rev. E: Stat. Phys., Plasmas, Fluids, Relat. Interdiscip. Top.*, 2002, **65**, 041720.
16 J. Cviklinski, A. R. Tajbakhsh and E. M. Terentjev, *Eur. Phys. J. E*, 2002, **9**, 427–434.
17 S. Iamsaard, S. J. Aβhoff, B. Matt, T. Kudernac, J. J. L. M. Cornelissen, S. P. Fletcher and N. Katsonis, *Nat. Chem.*, 2014, **6**, 229–235.
18 Y. Yu, M. Nakano and T. Ikeda, *Nature*, 2003, **425**, 145.
19 M. Yamada, M. Kondo, J. I. Mamiya, Y. Yu, M. Kinoshita, C. J. Barrett and T. Ikeda, *Angew. Chem., Int. Ed.*, 2008, **47**, 4986–4988.
20 L. Wang and Q. Li, *Adv. Funct. Mater.*, 2016, **26**, 10–28.
21 L. Wang, H. Dong, Y. Li, R. Liu, Y.-F. Wang, H. K. Bisoyi, L.-D. Sun, C.-H. Yan and Q. Li, *Adv. Mater.*, 2015, **27**, 2065–2069.
22 L. Wang, K. G. Gutierrez-Cuevas, H. K. Bisoyi, J. Xiang, G. Singh, R. S. Zola, S. Kumar, O. D. Lavrentovich, A. Urbasd and Q. Li, *Chem. Commun.*, 2015, **51**, 15039–15042.
23 L. Wang, H. Dong, Y. Li, C. Xue, L.-D. Sun, C.-H. Yan and Q. Li, *J. Am. Chem. Soc.*, 2014, **136**, 4480–4483.
24 H. K. Bisoyi and Q. Li, *Acc. Chem. Res.*, 2014, **47**, 3184–3195.
25 W. Wu, L. Yao, T. Yang, R. Yin, F. Li and Y. Yu, *J. Am. Chem. Soc.*, 2011, **133**, 15810–15813.
26 Z. Jiang, M. Xu, F. Li and Y. Yu, *J. Am. Chem. Soc.*, 2013, **135**, 16446–16453.
27 L. Yang, K. Setyowati, A. Li, S. Gong and J. Chen, *Adv. Mater.*, 2008, **20**, 2271–2275.
28 J. E. Marshall, Y. Ji, N. Torras, K. Zinoviev and E. M. Terentjev, *Soft Matter*, 2012, **8**, 1570–1574.
29 N. Torras, K. E. Zinoviev, J. E. Marshall, E. M. Terentjev and J. Esteve, *Appl. Phys. Lett.*, 2011, **99**, 254102.
30 C. J. Camargo, H. Campanella, J. E. Marshall, N. Torras, K. Zinoviev, E. M. Terentjev and J. Esteve, *Macromol. Rapid Commun.*, 2011, **32**, 1953–1959.
31 C. Li, Y. Liu, X. Huang and H. Jiang, *Adv. Funct. Mater.*, 2012, **22**, 5166–5174.
32 R. R. Kohlmeyer and J. Chen, *Angew. Chem., Int. Ed.*, 2013, **52**, 9234–9237.
33 Y. Ji, Y. Y. Huang, R. Rungsawang and E. M. Terentjev, *Adv. Mater.*, 2010, **22**, 3436–3440.
34 M. Wang, S. Mir Sayed, L. X. Guo, B. P. Lin, X. Q. Zhang, Y. Sun and H. Yang, *Macromolecules*, 2016, **49**, 663–671.
35 J. S. Evans, Y. Sun, B. Senyuk, P. Keller, V. M. Pergamenshchik, T. Lee and I. I. Smalyukh, *Phys. Rev. Lett.*, 2013, **110**, 187802.
36 X. Liu, R. Wei, P. T. Hoang, X. Wang, T. Liu and P. Keller, *Adv. Funct. Mater.*, 2015, **25**, 3022–3032.
37 H. Yang, J. J. Liu, Z. F. Wang, L. X. Guo, P. Keller, B. P. Lin, Y. Sun and X. Q. Zhang, *Chem. Commun.*, 2015, **51**, 12126–12129.
38 M. Camacho-Lopez, H. Finkelmann, P. Palffy-Muhoray and M. Shelley, *Nat. Mater.*, 2004, **3**, 307–310.
39 C. L. M. Harvey and E. M. Terentjev, *Eur. Phys. J. E*, 2007, **23**, 185–189.
40 J. E. Marshall and E. M. Terentjev, *Soft Matter*, 2013, **9**, 8547–8551.
41 L. T. de Haan, C. Sanchez-Somolinos, C. M. W. Bastiaansen, A. P. H. J. Schenning and D. J. Broer, *Angew. Chem., Int. Ed.*, 2012, **51**, 12469–12472.
42 L. T. de Haan, V. Gimenez-Pinto, A. Konya, T.-S. Nguyen, J. M. N. Verjans, C. Sánchez-Somolinos, J. V. Selinger, R. L. B. Selinger, D. J. Broer and A. P. H. J. Schenning, *Adv. Funct. Mater.*, 2014, **24**, 1251–1258.
43 A. Boehm, W. Helfer, G. Beck, M. Krieger and P. Erk, WO, 076988, 2002.
44 M. Erkelenz, R. Wehrmann and A. Boumans, *US Pat.*, 0252282, 2014.
45 G. T. Spence, G. V. Hartland and B. D. Smith, *Chem. Sci.*, 2013, **4**, 4240–4244.
46 D. L. Thomsen, P. Keller, J. Naciri, R. Pink, H. Jeon, D. Shenoy and B. R. Ratna, *Macromolecules*, 2001, **34**, 5868–5875.
47 H. Yang, M. X. Liu, Y. W. Yao, P. Y. Tao, B. P. Lin, P. Keller, X. Q. Zhang, Y. Sun and L. X. Guo, *Macromolecules*, 2013, **46**, 3406–3416.
48 B. Geng, L. X. Guo, B. P. Lin, P. Keller, X. Q. Zhang, Y. Sun and H. Yang, *Polym. Chem.*, 2015, **6**, 5281–5287.
49 H. Yang, Y. J. Lv, M. Xu, J. Wang, B. P. Lin, L. X. Guo and E. Q. Chen, *Polym. Chem.*, 2015, **6**, 6709–6719.

50 A. Buguin, M. H. Li, P. Silberzan, B. Ladoux and P. Keller, *J. Am. Chem. Soc.*, 2006, **128**, 1088–1089.
51 H. Yang, A. Buguin, J. M. Taulemesse, K. Kaneko, S. Méry, A. Bergeret and P. Keller, *J. Am. Chem. Soc.*, 2009, **131**, 15000–15004.
52 E. Anglaret, M. Brunet, B. Desbat, P. Keller and T. Buffeteau, *Macromolecules*, 2005, **38**, 4799–4810.
53 X. Z. Song and J. W. Foley, *Dyes Pigm.*, 2008, **78**, 60–64.
54 T. Ikeda, M. Nakano, Y. L. Yu, O. Kanazawa and A. Tsutsumi, *Adv. Mater.*, 2003, **15**, 201–205.
55 M. H. Li, P. Keller, B. Li, X. Wang and M. Brunet, *Adv. Mater.*, 2003, **15**, 569–572.